

SymmCompletion: High-Fidelity and High-Consistency Point Cloud Completion with Symmetry Guidance

Hongyu Yan^{1*}, Zijun Li^{2*}, Kunming Luo¹, Li Lu^{2†}, Ping Tan^{1†}

¹Hong Kong University of Science and Technology

²Sichuan University

{hyanar, kluoad}@connect.ust.hk, lzj020524@gmail.com

luli@scu.edu.cn, pingtan@ust.hk

Abstract

Point cloud completion aims to recover a complete point shape from a partial point cloud. Although existing methods can form satisfactory point clouds in global completeness, they often lose the original geometry details and face the problem of geometric inconsistency between existing point clouds and reconstructed missing parts. To tackle this problem, we introduce **SymmCompletion**, a highly effective completion method based on symmetry guidance. Our method comprises two primary components: a Local Symmetry Transformation Network (LSTNet) and a Symmetry-Guidance Transformer (SGFormer). First, LSTNet efficiently estimates point-wise local symmetry transformation to transform key geometries of partial inputs into missing regions, thereby generating geometry-align partial-missing pairs and initial point clouds. Second, SGFormer leverages the geometric features of partial-missing pairs as the explicit symmetric guidance that can constrain the refinement process for initial point clouds. As a result, SGFormer can exploit provided priors to form high-fidelity and geometry-consistency final point clouds. Qualitative and quantitative evaluations on several benchmark datasets demonstrate that our method outperforms state-of-the-art completion networks.

Code —

<https://github.com/HongyuYann/SymmCompletion.git>

Introduction

As a fundamental 3D representation, point clouds are widely used in fields such as autonomous driving, augmented reality, and robotics. However, due to occlusion and resolution limitations of devices, point clouds captured by LiDAR and depth cameras are often sparse and incomplete. These low-quality point clouds hinder the research and development of upstream tasks, such as point cloud classification (Qi et al. 2017a), segmentation (Qi et al. 2017b), and detection (Wu, Qi, and Fuxin 2019). Consequently, point cloud completion has become a crucial task aimed at improving data quality by reconstructing complete and detailed point clouds from partial observations.

Existing point cloud completion methods generally follow two distinct strategies: reconstructing either the entire point cloud or only the missing regions. The former strategy typically begins by predicting a coarse but complete point skeleton, which is then refined using an upsampling method. However, these methods often struggle to generate high-fidelity results. The extremely sparse point skeletons predicted from global features face challenges in preserving the original geometric structures, making it difficult for the refinement network to recover detailed point clouds. As a result, even certain geometries present in the partial inputs may not be reconstructed. To avoid the loss of original geometries, other methods (Huang et al. 2020; Yu et al. 2021; Li et al. 2023b) that follow the latter strategy focus on recovering only the geometries of the missing regions. Although this approach ensures completion fidelity by shifting the learning goal, it struggles to produce consistent results due to the lack of global optimization. Additionally, these methods often suffer from uneven distribution between the existing regions and the missing ones. Recent methods (Mendoza et al. 2020; Zhang et al. 2023a) have introduced a refining process to globally optimize the combination of partial point clouds and missing regions. However, they still face issues with insufficient consistency because their simplistic approaches to global optimization fail to capture precise geometric information necessary for effective refinement.

In this paper, we propose a novel method called SymmCompletion to enhance completion fidelity and consistency. As illustrated in Figure 1, following the latter strategy, SymmCompletion first reconstructs the missing parts and then applies a global optimization network to refine the initial point cloud. Our core solution involves two key approaches: first, enhancing the geometric consistency of the predicted missing parts; and second, providing explicit geometric guidance for global optimization to improve the capabilities of geometric preservation and restoration.

Specifically, we found that the symmetry of 3D models is beneficial for obtaining high-consistency missing parts. However, previous symmetry-based methods struggle to produce accurate missing regions because the global transformations they apply fail to achieve symmetry in local regions. To address this, we propose a Local Symmetry Transformation Network (LSTNet) to leverage local symmetry information for constructing high-quality missing parts. The

*These authors contributed equally.

†Corresponding author.

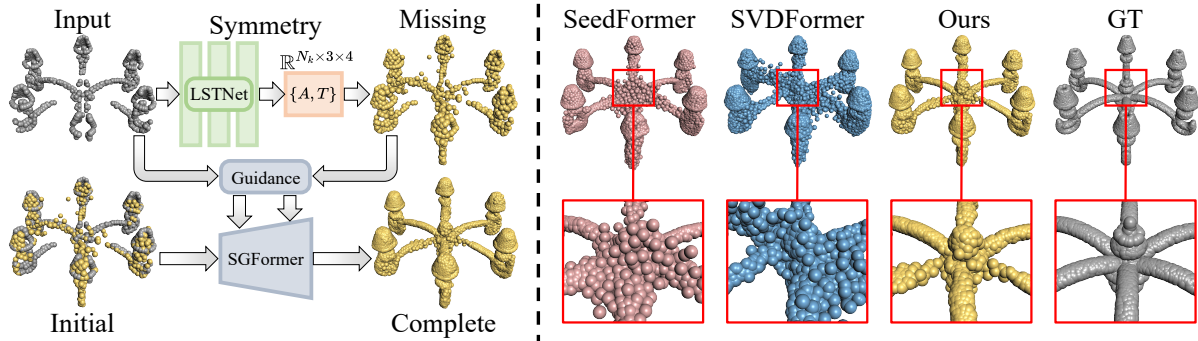


Figure 1: The overview structure of our SymmCompletion (**left**) and visual comparison (**right**) with recent state-of-the-art works SeedFormer (Zhou et al. 2022) and SVDFormer (Zhu et al. 2023). SymmCompletion starts to conduct a partial-missing pair and an initial point cloud and then uses the symmetry information existing in this pair to guide the refinement of the initial point cloud. With the help of symmetry guidance, SymmCompletion generates high-fidelity and high-consistency results.

key insight is to estimate point-wise symmetry transformations for each point using local point features. This symmetry transformation consists of a point-wise affine matrix and a translation matrix, which are used to transform key geometric points of partial inputs to the missing regions based on symmetry. In this way, LSTNet can complete high-consistency missing areas by effectively migrating existing geometric structures.

After obtaining partial-missing pairs, we aim to use their geometries to guide the refining process and improve completion fidelity. Due to asymmetry and significant geometric deficiencies in certain partial inputs, hollow and discontinuous regions often appear in the initial combination of partial-missing pairs, particularly at the connections between existing and missing parts. Thus, symmetric geometry guidance is essential for our global optimization. To address this, we introduce a novel Symmetry-Guidance Transformer (SGFormer), which leverages symmetry guidance. Specifically, SGFormer uses the geometric information of partial-missing pairs to ensure the network focuses on preserving existing structures and refining hollow and discontinuous areas. We design a dual-path perception mechanism with attention to integrate geometric features of partial-missing pairs into the features of the refining process inputs. Consequently, SGFormer explicitly applies symmetric priors as guidance to produce final results, thereby enhancing completion fidelity and consistency. We conducted quantitative and qualitative experiments on several widely used datasets to demonstrate that our SymmCompletion achieves state-of-the-art performance compared to existing methods. Our main contributions are summarized as follows:

- We present a novel framework, SymmCompletion, for point cloud completion to enhance geometric fidelity and consistency. This framework achieves state-of-the-art performance on multiple completion benchmarks.
- We propose LSTNet to generate geometry-aligned missing parts. Rather than relying on global symmetry, we estimate point-wise affine and translation matrices from point features to achieve local symmetry transformation.

- We further developed SGFormer to optimize the initial point clouds. By incorporating symmetric guidance derived from the geometric information of partial-missing pairs, SGFormer effectively preserves existing geometric structures and refines hollow and discontinuous areas.

Related Work

3D Point Cloud Completion

Existing point cloud completion methods can be categorized into two main approaches: reconstructing the entire point cloud or focusing solely on the missing regions.

Overall point cloud. Based on MLPs, the pioneering method PCN (Yuan et al. 2018) proposed a coarse-to-fine completion framework. It first predicts a sparse but complete point cloud via an auto-encoder structure, then uses a folding operation (Yang et al. 2018) to upsample and refine the predicted coarse point cloud. Building on this pipeline, subsequent methods achieved a series of advanced improvements. Several methods (Xie et al. 2020; Wang, Ang, and Lee 2021; Huang et al. 2021; Liu et al. 2020; Pan et al. 2021; Wang, Ang Jr, and Lee 2020; Tchapmi et al. 2019; Wen et al. 2021) proposed extracting detailed features to aid completion by introducing effective techniques in the 3D point cloud processing (Wang et al. 2019b; Wu, Qi, and Fuxin 2019). With the success of Transformer (Dosovitskiy et al. 2020; Guo et al. 2021; Zhao et al. 2021), recent approaches (Li et al. 2023b; Fu et al. 2023; Zhou et al. 2022) used attention mechanisms to further enhance network perception of detailed geometries. For instance, SnowflakeNet (Xiang et al. 2021) and FBNet (Yan et al. 2022) introduced a skip-transformer and a cross-transformer, respectively, to address the local feature fusion problem. However, these methods often discard information-rich inputs to produce new, information-poor point skeletons, leading to the loss of existing detailed structural information. As a result, despite designing powerful refinement networks, these methods struggle to generate high-fidelity complete point clouds.

Only the missing regions. To avoid the loss of the original structure of partial inputs, another category of meth-

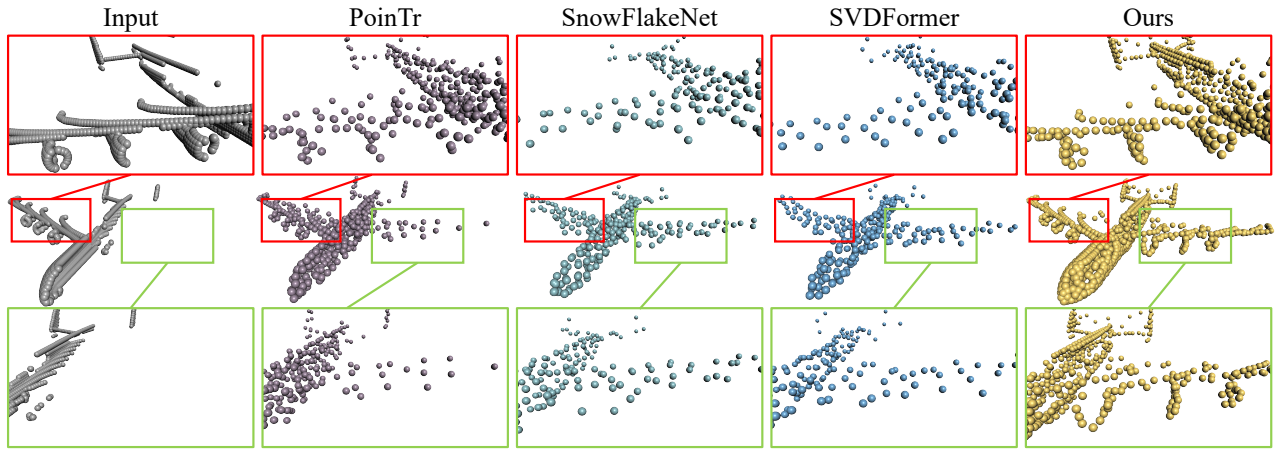


Figure 2: Visualization of initial point clouds from our LSTNet and previous methods, including PoinTr (Yu et al. 2021), SnowflakeNet (Xiang et al. 2021), and SVDFormer (Zhu et al. 2023). Our LSTNet not only maintains existing geometries but also reconstructs high-consistency missing parts through local symmetry transformation, distinguishing it from previous methods.

ods (Huang et al. 2020; Yu et al. 2021; Li et al. 2023b; Chen et al. 2023a) focuses on estimating only the missing regions. The final results are obtained by combining the partial inputs with the reconstructed missing regions. For example, PF-Net (Huang et al. 2020) utilized a hierarchical network to progressively generate missing parts. PoinTr (Yu et al. 2021) approached point cloud completion as a set-to-set translation problem, employing transformers to generate the translation from partial to complete parts. However, due to the lack of global optimization for the final results, these methods often suffer from uneven distribution between existing regions and missing ones. In cases with complicated geometric structures, these methods are prone to forming shapes with holes and crevices.

Application of symmetry priors

Symmetry is an important property in our world, and many methods (Zhang et al. 2023b; Ma et al. 2023; Rumezhak et al. 2021; Li et al. 2023a; Zhao et al. 2023; Fan et al. 2023; Wang et al. 2019a) have utilized this cue to enhance their approaches. For example, NeRD (Zhou, Liu, and Ma 2021) presented a neural 3D reflection symmetry detector to recover the normal direction of objects’ mirror planes. In the area of point cloud completion, there are several methods (Schiebener et al. 2016; Cui et al. 2023) applied the symmetry priors to obtain the missing part. For instance, USSPA (Ma et al. 2023) designed a symmetry generation module to obtain symmetric parts for an incomplete point cloud, assuming that all objects are axisymmetric and the symmetric plane is perpendicular to the xz -plane and zero-crossing. GTNet (Zhang et al. 2023a) exploited global features extracted from partial inputs to form a global transformation matrix, rotating the whole point cloud to gain missing parts. However, these completion methods face challenges in generating high-quality missing parts. On one hand, the simple axisymmetric assumption is limited and cannot accommodate non-axisymmetric objects. On the

other hand, the global transformation matrix rotates the entire point cloud to another plane, which fails to address symmetry in local regions. Consequently, these methods struggle to generate high-consistency symmetric parts.

Method

The overall architecture of our SymmCompletion is shown in Figure 1. First, we use our Local Symmetry Transformation Network (LSTNet) to generate high-consistency partial-missing pairs and initial point clouds. Then, we design a Symmetry-Guidance Transformer (SGFormer) to form high-fidelity complete point clouds by leveraging the partial-missing pairs to guide the point cloud refining process.

Local Symmetry Transformation Network

In this stage, our goal is to generate high-consistency missing parts whose geometries align as closely as possible with the partial input. To achieve this, we propose a novel Local Symmetry Transformation Network (LSTNet), which focuses on learning point-wise symmetry transformations to map the existing geometries of the partial input into the missing regions. This approach reconstructs a high-consistency and high-fidelity initial point cloud. As shown in Figure 3, previous methods (Yu et al. 2021; Xiang et al. 2021; Zhu et al. 2023) failed to reconstruct high-consistency missing parts (see the bottom) and lost existing geometric information (see the top). In contrast, our LSTNet avoids these drawbacks through local point-wise symmetry transformation.

Specifically, as shown in Figure 3, LSTNet first utilizes a down-sampling network to extract the input’s key geometries $P_k \in \mathbb{R}^{N_k \times 3}$, corresponding point features $F_k \in \mathbb{R}^{N_k \times C}$ and global features $g \in \mathbb{R}^{1 \times C}$, here N_k and C is the number of points and channels. This down-sampling network consists of a set abstraction layer (Qi et al. 2017b), a point transformer (Zhao et al. 2021), and a feature expansion

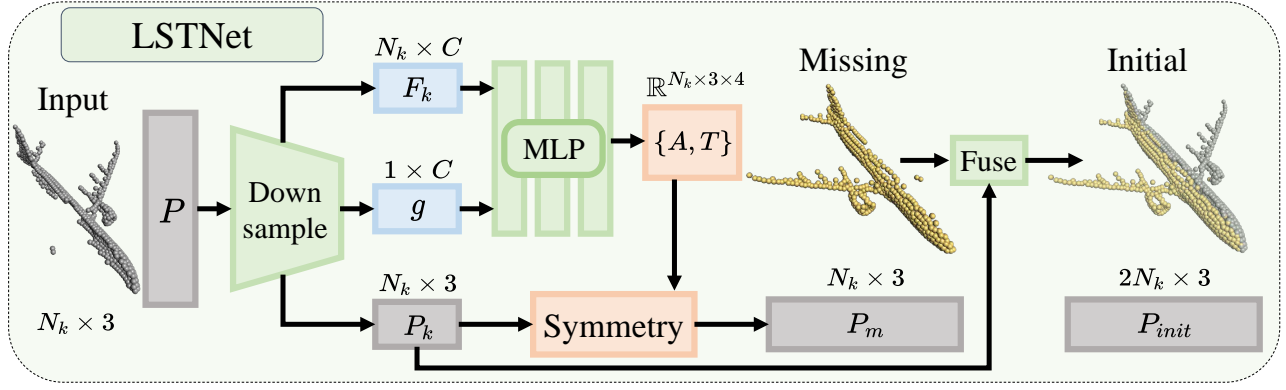


Figure 3: The structure of LSTNet. Given a partial input, we first extract key geometries P_k , key features F_k , and global features g . Then we use an MLP to predict point-wise affine matrix A and translation matrix T to turn the key geometries P_k into missing part P_m . Finally, we gain the initial point cloud P_{init} and partial-missing pairs.

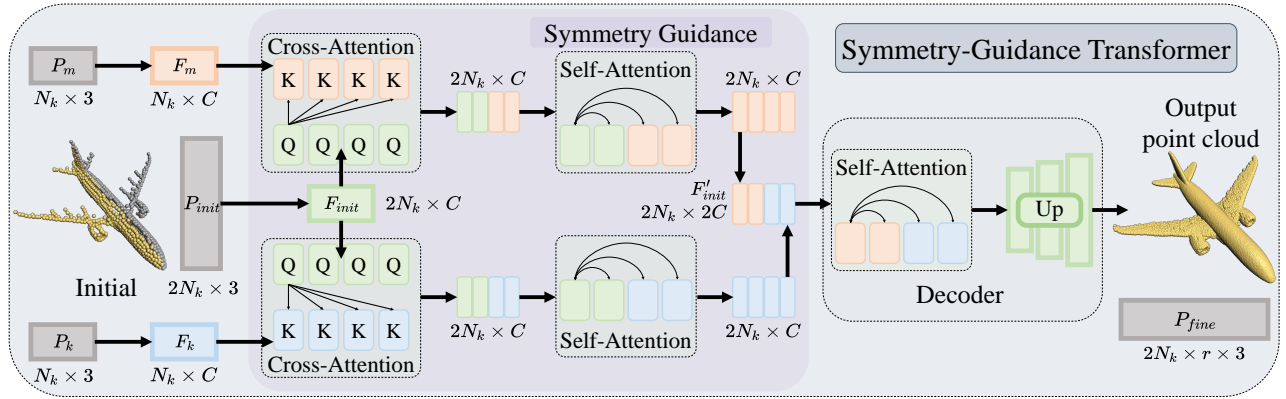


Figure 4: The overall architecture of Symmetry-Guidance Transformer (SGFormer). Given the features F_k of key geometries P_k of partial inputs, F_m of missing parts of points P_m , and F_{init} of initial points P_{init} , SGFormer leverage dual-path perception based on cross-attention and self-attention layers to guide the refinement of initial point clouds to form geometry-consistency results.

sion layer. Detailed information about the down-sampling network can be found in the supplementary material. After down-sampling, we combine the local features of each point with the global features to estimate point-wise symmetry transformations using a series of MLPs and reshaping operations. Since the global features can obtain information on global symmetry and global perception, we use them to enhance the estimation of symmetry transformation. Our local symmetry transformation is composed of a point-wise affine matrix $A \in \mathbb{R}^{N_k \times 3 \times 3}$ and a point-wise translation matrix $T \in \mathbb{R}^{N_k \times 3}$. Thus, we can define our local symmetry transformation as follows:

$$P_m = P_k Q\{\mathcal{M}(F)\} + \mathcal{N}(F) \quad (1)$$

where \mathcal{M} and \mathcal{N} are MLPs for predicting the affine matrix A and the translation matrix T , respectively. Q denotes the reshaping operation that is used to convert the channel of the affine matrix to the $\mathbb{R}^{3 \times 3}$ matrix. $P_m \in \mathbb{R}^{N_k \times 3}$ is the produced missing parts relative to input P_k .

Finally, we concatenate P_k and P_m to gain our initial

point cloud P_{init} , which can be defined as follows:

$$P_{init} = [P_k, P_m] \quad (2)$$

where $[\cdot]$ is the operation of concatenation.

Symmetry-Guidance Transformer

After obtaining the partial-missing pairs, we use the symmetric information to guide the refinement process for initial point clouds, aiming to form high-fidelity final results. To achieve this, we propose a Symmetry-Guidance Transformer (SGFormer). As shown in Figure 4, SGFormer first extracts the features $F_{init} \in \mathbb{R}^{2N_k \times C}$ of the initial point clouds $P_{init} \in \mathbb{R}^{2N_k \times 3}$. Following previous methods (Xiang et al. 2021; Zhou et al. 2022), we use several MLPs and a max-pooling operation to obtain local features and global features of the initial point cloud P_{init} . Then, we use the point transformer (Zhao et al. 2021) to gain the geometric features F_{init} . We also use this way to obtain the features $F_m \in \mathbb{R}^{N_k \times C}$ of the missing parts P_m .

Then, we gain three point features, including feature F_m of missing parts P_m , feature F_k of key geometries P_k of

Methods	Airplane	Cabinet	Car	Chair	Lamp	Sofa	Table	Watercraft	CD-AVG (\downarrow)	F1 (\uparrow)
PCN (Yuan et al. 2018)	5.50	22.70	10.63	8.70	11.00	11.34	11.68	8.59	9.64	0.695
PoinTr (Yu et al. 2021)	4.75	10.47	8.68	9.39	7.75	10.93	7.78	7.29	8.38	-
SnowflakeNet (Xiang et al. 2021)	4.29	9.16	8.08	7.89	6.07	9.23	6.55	6.40	7.21	0.801
FBNet (Yan et al. 2022)	3.99	9.05	7.90	7.38	5.82	8.85	6.35	6.18	6.94	-
SeedFormer (Zhou et al. 2022)	3.85	9.05	8.06	7.06	5.21	8.85	6.05	5.58	6.74	0.818
SVDFormer (Zhu et al. 2023)	3.62	8.79	7.46	6.91	5.33	8.49	5.90	5.83	6.54	0.841
GTNet (Zhang et al. 2023a)	4.17	9.33	8.38	7.66	5.49	9.44	6.69	6.07	7.15	-
AnchorFormer (Chen et al. 2023b)	3.70	8.94	7.57	7.05	5.21	8.40	6.03	5.81	6.59	-
CRA-PCN (Rong et al. 2024)	3.59	8.70	7.50	6.70	5.06	8.24	5.72	5.64	6.39	-
SymmCompletion	3.53	8.49	7.30	6.52	5.06	8.23	5.64	5.49	6.28	0.853

Table 1: Quantitative results in terms of $l1$ Chamfer Distance $\times 10^3$ (CD) and F1-Score@%1 (F1) on PCN dataset.

Method	2048		4096		8192		16384	
	CD (\downarrow)	F1 (\uparrow)	CD (\downarrow)	F1 (\uparrow)	CD (\downarrow)	F1 (\uparrow)	CD (\downarrow)	F1 (\uparrow)
PCN (Yuan et al. 2018)	9.77	0.320	7.96	0.458	6.99	0.563	6.02	0.638
CRN (Wang, Ang Jr, and Lee 2020)	7.25	0.434	5.83	0.569	4.90	0.680	4.30	0.740
VRCNet (Pan et al. 2021)	5.96	0.499	4.70	0.636	3.64	0.727	3.12	0.791
PoinTr (Yu et al. 2021)	-	-	5.18	0.606	3.94	0.724	3.08	0.767
SnowflakeNet (Xiang et al. 2021)	5.71	0.503	4.40	0.661	3.48	0.743	2.73	0.796
FBNet (Yan et al. 2022)	5.06	0.532	3.88	0.671	2.99	0.766	2.29	0.822
GTNet (Zhang et al. 2023a)	5.76	-	4.18	-	3.05	-	2.19	-
SymmCompletion	4.89	0.534	3.65	0.691	2.70	0.782	2.14	0.850

Table 2: Quantitative results in terms of L2 Chamfer Distance $\times 10^4$ (CD) and F1-score@%1 (F1) on the MVP dataset with different resolutions.

partial inputs, and feature F_{init} of initial point cloud P_{init} , here F_k comes from the down-sampling network in STNet. To introduce symmetry information as explicit signals to guide the refinement process, we design dual-path perception with the attention mechanism, one path for the partial point clouds P_k and another for the missing parts P_m . Following existing methods (Hong et al. 2023; Jiang et al. 2023) applied in the 3D generation, we fuse cross-attention and self-attention mechanisms to aggregate features. As shown in Figure 4, give the features F_k , F_m , F_{init} , we gain the corresponding fused features F_{init}^k and F_{init}^m by considering F_{init} as query tokens. After that, we gain the dual-path fusion features $F'_{init} \in \mathbb{R}^{2N_k \times 2C}$ by combining F_{init}^k and F_{init}^m . We can define our feature fusion as follows:

$$F'_{init} = [\phi(F_{init}, F_k), \beta(F_{init}, F_m)] \quad (3)$$

where ϕ and β are combinations of cross-attention and self-attention layers.

Finally, we use a decoder to form the refined complete point clouds from combined features F'_{init} . In this decoder, we first apply two self-attention layers to enhance fusion features F'_{init} . Compared with using MLPs to decode directly, those two self-attention layers can improve the network to preserve the features of partial-missing pairs while perceiving those incomplete and discontinuous regions. Afterward, we use a point-shuffle operation composed of MLPs and the reshaping operation to predict point offsets. The point-shuffle operation can form offsets with an upsampling ratio r for each point to upsample the original input. Subsequently, we obtain the refined point cloud P_f by adding the offset to the points of the input point cloud. The refined point cloud

can be defined as:

$$P_{fine} = \mathcal{R}(P_{init}) + \mathcal{S}(\theta(F'_{init})). \quad (4)$$

where θ represents two self-attention layers. \mathcal{R} and \mathcal{S} are repeated operation and point-shuffle operation, respectively. Based on the coarse-to-fine pipeline, we stack two SGFormers with different upsampling ratios to reconstruct final point clouds progressively.

Loss Function

We use the Chamfer Distance (CD) as our main distance function, which calculates the average closest point distances between the output and the ground truth. For the end-to-end training on our SymmCompletion, the total loss function can be formulated as:

$$\mathcal{L} = \mathcal{L}_{CD}(P', Q) + \sum_{i=1}^n \mathcal{L}_{CD}(P_i, Q), \quad (5)$$

where P' and P_i denote the initial and fine output of each SGFormer, respectively, Q is the ground truth. n is the number of SGFormers.

Experiments

In this section, we first introduce the datasets and evaluation metrics for the point cloud completion task. Then, we compare our method with previous methods on several datasets and provide the visualized analysis.

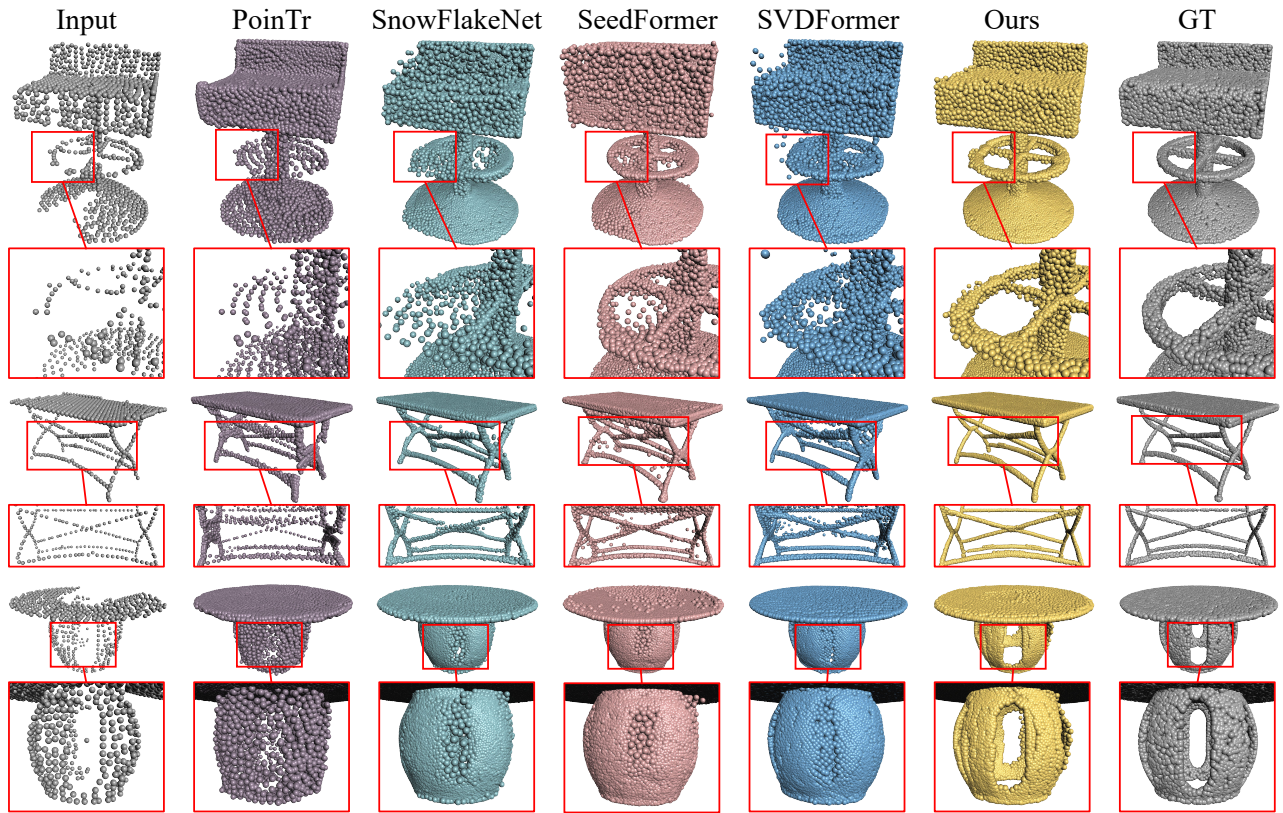


Figure 5: Visualization of results on the PCN dataset (Yuan et al. 2018). As emphasized by the zoom-in views, our SymmCompletion presents a better performance in terms of completion fidelity and consistency compared with previous methods (Xiang et al. 2021; Yu et al. 2021; Zhou et al. 2022; Zhu et al. 2023).

Datasets and Evaluation Metric

In our experiment, we use three widely adopted synthetic datasets for training and evaluation, including the **PCN dataset** (Yuan et al. 2018), **MVP dataset** (Pan et al. 2021), and **ShapeNet55/34 dataset** (Yu et al. 2021). Additionally, we test our method on the KITTI (Geiger et al. 2013) dataset to evaluate the network’s generalization ability in real-world scenarios. Following previous methods, we apply the F1-score and CD with l_1 and l_2 norm as metrics to compare our method with the previous methods on synthetic datasets.

Comparison to the state-of-the-art

In this section, we first present the quantitative results of the (L_1) norm of Chamfer Distance (CD) and F1-score on the PCN dataset in Table 1. Our SymmCompletion achieves the best CD performance in each category and the best average values for both CD and F1-score across all categories. In addition to quantitative comparisons, we also provide visualized results in Figure 5. As shown in the figure, our SymmCompletion generates high-fidelity and high-consistency results. Specifically, SymmCompletion not only preserves original geometries but also recovers geometry-consistent missing parts. For instance, in the first sample, previous methods fail to reconstruct accurate geometries in

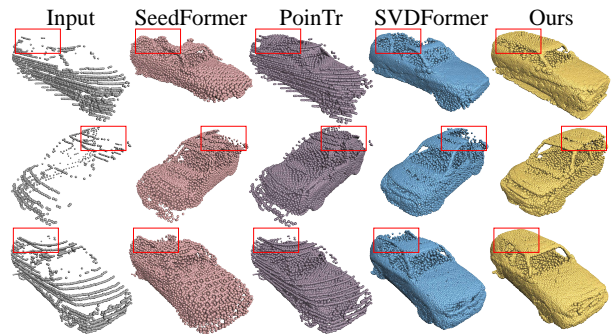


Figure 6: Visualization of results on the KITTI dataset. Compared with recent methods (Yu et al. 2021; Zhou et al. 2022; Zhu et al. 2023), our SymmCompletion presents a better performance in terms of completion completeness (see **highlight regions**).

the highlighted regions. In the second and last samples, these methods lose the original geometries. In contrast, SymmCompletion produces superior results.

Table 2 provides a quantitative comparison of our method against others at four different resolutions on the MVP dataset, indicating that our SymmCompletion can generate

Method	ShapeNet 55 dataset			34 seen categories			21 unseen categories		
	CD-S (\downarrow)	CD-M (\downarrow)	CD-H (\downarrow)	CD-S (\downarrow)	CD-M (\downarrow)	CD-H (\downarrow)	CD-S (\downarrow)	CD-M (\downarrow)	CD-H (\downarrow)
PCN (Yuan et al. 2018)	1.94	1.96	4.08	1.87	1.81	2.97	3.17	3.08	5.29
PoinTr (Yu et al. 2021)	0.58	0.88	1.79	0.76	1.05	1.88	1.04	1.67	3.44
SeedFormer (Zhou et al. 2022)	0.50	0.77	1.49	0.48	0.70	1.30	0.61	1.07	2.35
SDNet (Chen et al. 2023a)	0.48	0.69	1.39	0.49	0.67	1.27	0.64	1.02	2.32
SVDFormer (Zhu et al. 2023)	0.48	0.70	1.30	0.46	0.64	1.13	0.61	1.05	2.19
GTNet (Zhang et al. 2023a)	0.45	0.66	1.30	0.51	0.73	1.40	0.78	1.22	2.56
CRA-PCN (Rong et al. 2024)	0.48	0.71	1.37	0.45	0.65	1.18	0.55	0.97	2.19
SymmCompletion	0.34	0.54	1.18	0.33	0.48	1.00	0.39	0.70	1.83

Table 3: Quantitative results in terms of L2 Chamfer Distance $\times 10^3$ (CD) on the ShapeNet55/34 (Yu et al. 2021) dataset for three difficulty levels.

Methods	PoinTr	SeedFormer	SVDFormer	Ours
FD (\downarrow)	0.0	1.45	11.3	2.54
MMD (\downarrow)	8.21	1.09	0.97	1.72

Table 4: Quantitative comparison on the KITTI dataset in terms of Fidelity Distance (FD) and Minimal Matching Distance (MMD)

high-quality complete point clouds across various resolutions. Furthermore, we test the performance of SymmCompletion on the ShapeNet55 dataset. As shown in Table 3, we report CD values for each method at simple (CD-S), median (CD-M), and hard (CD-H) levels. SymmCompletion outperforms previous methods across all levels. Additionally, following previous methods (Yu et al. 2021; Zhu et al. 2023), we study the generalization capability of SymmCompletion on the 34 seen categories and 21 unseen categories. From these experiments, we find that SymmCompletion demonstrates a higher generalization capability compared to previous methods.

Finally, we test our method on real-world datasets. Following previous methods (Zhou et al. 2022), we directly evaluate the model trained on PCN’s dataset (Yuan et al. 2018) by using the metrics of the Fidelity Distance (FD) and Minimal Matching Distance (MMD). The quantitative comparison is presented in Table 4. Although our SymmCompletion doesn’t obtain the best performance in the FD and MMD metrics, it presents a better visual performance in terms of completion completeness, as shown in Figure 6. In the highlighted regions, SymmCompletion reconstructs more complete and accurate structures than previous methods. It is worth noting that the domain and scale gap between the KITTI dataset and PCN’s dataset affects the fairness and accuracy of quantitative comparisons. For example, the FD metric computes the single-sided Chamfer Distance. If we concatenate the partial inputs into the final outputs, we will obtain a zero FD, as seen with PoinTr. Additionally, if we preserve the geometries of KITTI’s inputs more, we will get higher MMD values. This is because certain geometries, such as ground points, do not exist in PCN’s cars. While the recovery of ground geometries indicates high generalization and fidelity of the model, it results in a large MMD metric value. We argue that the quantitative comparison on the ShapeNet-21 dataset is more suitable to indicate our superiority for generalizability.

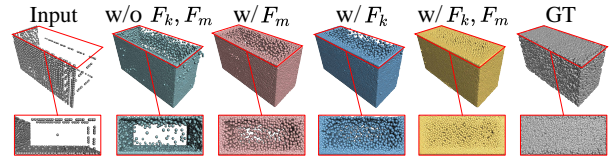


Figure 7: Visualized comparison for symmetry guidance.

Features F_k	Features F_m	CD (\downarrow)	F1 (\uparrow)
		6.51	0.839
✓		6.45	0.842
	✓	6.37	0.849
✓	✓	6.28	0.853

Table 5: The effect of symmetry guidance in our SGFormer.

In summary, our method achieves impressive improvements on these four datasets. We argue that this mainly comes from our symmetry guidance and local symmetry.

Ablation Study

Ablation for symmetry guidance

In this section, we investigate the effects of symmetry guidance. Specifically, we remove the features F_k of key geometries from partial inputs and the features F_m from formed missing parts, respectively. As shown in Table 5, our SymmCompletion achieves the best performance with features F_k and F_m . We also provide a qualitative comparison shown in Figure 7. This ablation study indicates that SGFormer can derive symmetry priors from the features of partial-missing pairs, enhancing the refinement of initial point clouds and thereby improving both completion consistency and fidelity.

Ablation for local symmetry transformation

To generate high-quality missing parts based on symmetry, we utilize local point features to estimate point-wise symmetry transformations for each point. In this ablation study, we aim to demonstrate the superiority of our STNet. Specifically, within the SymmCompletion architecture, we replace our STNet with two alternative models for quantitative comparison. For the first model, we follow USSPA (Ma et al. 2023) to predict symmetric arguments A using global features, subsequently obtaining the missing parts P_m through operation: $P_m = P - 2 \frac{A \cdot P}{\|A\|^2} A$. For the second model, we

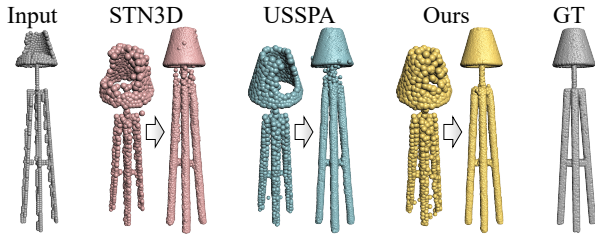


Figure 8: Visualized initial output (**left**) and the final result (**right**) for different symmetry transformations.

Model	USSPA	STN3D	LSTNet
CD (\downarrow)	6.51	6.48	6.28
F1 (\uparrow)	0.839	0.842	0.853

Table 6: The quantitative comparison for different symmetry transformations.

follow GTNet (Zhang et al. 2023a) and use their global-symmetry-based STN3D to estimate missing regions. The quantitative and qualitative results presented in Table 6 and Figure 8 indicate that our LSTNet is more effective for obtaining missing parts through symmetry transformation.

Conclusion

In conclusion, we introduce a novel framework for point cloud completion. Leveraging geometry guidance, our SymmCompletion achieves both high-fidelity and high-consistency completion. The proposed Symmetry Transformation Network (STNet) estimates local symmetry, enhancing the accuracy of the generated missing parts to form high-consistency partial-missing pairs. Subsequently, our Symmetry-Guidance Transformer (SGFormer) improves completion fidelity and consistency between reconstructed shapes and partial inputs by explicitly utilizing symmetry information in partial-missing pairs as guidance. Extensive experiments on various completion benchmarks demonstrate that our method outperforms state-of-the-art approaches.

References

Chen, J.; Liu, Y.; Liang, Y.; Long, D.; He, X.; and Li, R. 2023a. SD-Net: Spatially-Disentangled Point Cloud Completion Network. In *Proceedings of the 31st ACM International Conference on Multimedia*, 1283–1293.

Chen, Z.; Long, F.; Qiu, Z.; Yao, T.; Zhou, W.; Luo, J.; and Mei, T. 2023b. Anchorformer: Point cloud completion from discriminative nodes. In *Proceedings of the IEEE/CVF conference on computer vision and pattern recognition*, 13581–13590.

Cui, R.; Qiu, S.; Anwar, S.; Liu, J.; Xing, C.; Zhang, J.; and Barnes, N. 2023. P2c: Self-supervised point cloud completion from single partial clouds. In *Proceedings of the IEEE/CVF International Conference on Computer Vision*, 14351–14360.

Dosovitskiy, A.; Beyer, L.; Kolesnikov, A.; Weissenborn, D.; Zhai, X.; Unterthiner, T.; Dehghani, M.; Minderer, M.;

Heigold, G.; Gelly, S.; et al. 2020. An image is worth 16x16 words: Transformers for image recognition at scale. *arXiv preprint arXiv:2010.11929*.

Fan, Z.; Zhang, Z.; Yang, S.; Zhong, C.; Cao, M.; and Xia, S. 2023. Unpaired Multi-domain Attribute Translation of 3D Facial Shapes with a Square and Symmetric Geometric Map. In *Proceedings of the IEEE/CVF International Conference on Computer Vision*, 20828–20838.

Fu, Z.; Wang, L.; Xu, L.; Wang, Z.; Laga, H.; Guo, Y.; Bous-said, F.; and Bennamoun, M. 2023. VAPCNet: Viewpoint-Aware 3D Point Cloud Completion. In *Proceedings of the IEEE/CVF International Conference on Computer Vision (ICCV)*, 12108–12118.

Geiger, A.; Lenz, P.; Stiller, C.; and Urtasun, R. 2013. Vision meets robotics: The kitti dataset. *The International Journal of Robotics Research*, 32(11): 1231–1237.

Guo, M.-H.; Cai, J.-X.; Liu, Z.-N.; Mu, T.-J.; Martin, R. R.; and Hu, S.-M. 2021. Pct: Point cloud transformer. *Computational Visual Media*, 7: 187–199.

Hong, Y.; Zhang, K.; Gu, J.; Bi, S.; Zhou, Y.; Liu, D.; Liu, F.; Sunkavalli, K.; Bui, T.; and Tan, H. 2023. Lrm: Large reconstruction model for single image to 3d. *arXiv preprint arXiv:2311.04400*.

Huang, T.; Zou, H.; Cui, J.; Yang, X.; Wang, M.; Zhao, X.; Zhang, J.; Yuan, Y.; Xu, Y.; and Liu, Y. 2021. Rfnet: Recurrent forward network for dense point cloud completion. In *Proceedings of the IEEE/CVF International Conference on Computer Vision*, 12508–12517.

Huang, Z.; Yu, Y.; Xu, J.; Ni, F.; and Le, X. 2020. Pf-net: Point fractal network for 3d point cloud completion. In *Proceedings of the IEEE/CVF Conference on Computer Vision and Pattern Recognition*, 7662–7670.

Jiang, H.; Jiang, Z.; Zhao, Y.; and Huang, Q. 2023. Leap: Liberate sparse-view 3d modeling from camera poses. *arXiv preprint arXiv:2310.01410*.

Li, R.-W.; Zhang, L.-X.; Li, C.; Lai, Y.-K.; and Gao, L. 2023a. E3Sym: Leveraging E (3) invariance for unsupervised 3D planar reflective symmetry detection. In *Proceedings of the IEEE/CVF International Conference on Computer Vision*, 14543–14553.

Li, S.; Gao, P.; Tan, X.; and Wei, M. 2023b. ProxyFormer: Proxy Alignment Assisted Point Cloud Completion with Missing Part Sensitive Transformer. In *Proceedings of the IEEE/CVF Conference on Computer Vision and Pattern Recognition*, 9466–9475.

Liu, M.; Sheng, L.; Yang, S.; Shao, J.; and Hu, S.-M. 2020. Morphing and sampling network for dense point cloud completion. In *Proceedings of the AAAI Conference on Artificial Intelligence*, 11596–11603.

Ma, C.; Chen, Y.; Guo, P.; Guo, J.; Wang, C.; and Guo, Y. 2023. Symmetric Shape-Preserving Autoencoder for Unsupervised Real Scene Point Cloud Completion. In *Proceedings of the IEEE/CVF Conference on Computer Vision and Pattern Recognition*, 13560–13569.

Mendoza, A.; Apaza, A.; Sipiran, I.; and Lopez, C. 2020. Refinement of predicted missing parts enhance point cloud completion. *arXiv preprint arXiv:2010.04278*.

- Pan, L.; Chen, X.; Cai, Z.; Zhang, J.; Zhao, H.; Yi, S.; and Liu, Z. 2021. Variational Relational Point Completion Network. In *Proceedings of the IEEE/CVF Conference on Computer Vision and Pattern Recognition*, 8524–8533.
- Qi, C. R.; Su, H.; Mo, K.; and Guibas, L. J. 2017a. Pointnet: Deep learning on point sets for 3d classification and segmentation. In *Proceedings of the IEEE conference on computer vision and pattern recognition*, 652–660.
- Qi, C. R.; Yi, L.; Su, H.; and Guibas, L. J. 2017b. Pointnet++: Deep hierarchical feature learning on point sets in a metric space. *Advances in neural information processing systems*, 30.
- Rong, Y.; Zhou, H.; Yuan, L.; Mei, C.; Wang, J.; and Lu, T. 2024. CRA-PCN: Point Cloud Completion with Intra- and Inter-level Cross-Resolution Transformers. *Proceedings of the AAAI Conference on Artificial Intelligence*.
- Rumezhakh, T.; Doboševych, O.; Hryniv, R.; Selotkin, V.; Karpiv, V.; and Maksymenko, M. 2021. Towards realistic symmetry-based completion of previously unseen point clouds. In *Proceedings of the IEEE/CVF International Conference on Computer Vision*, 2542–2550.
- Schiebener, D.; Schmidt, A.; Vahrenkamp, N.; and Asfour, T. 2016. Heuristic 3D object shape completion based on symmetry and scene context. In *2016 IEEE/RSJ International Conference on Intelligent Robots and Systems (IROS)*, 74–81. IEEE.
- Tchapmi, L. P.; Kosaraju, V.; Rezatofighi, H.; Reid, I.; and Savarese, S. 2019. Topnet: Structural point cloud decoder. In *Proceedings of the IEEE/CVF Conference on Computer Vision and Pattern Recognition*, 383–392.
- Wang, W.; Ceylan, D.; Mech, R.; and Neumann, U. 2019a. 3dn: 3d deformation network. In *Proceedings of the IEEE/CVF Conference on Computer Vision and Pattern Recognition*, 1038–1046.
- Wang, X.; Ang, M. H.; and Lee, G. H. 2021. Voxel-based network for shape completion by leveraging edge generation. In *Proceedings of the IEEE/CVF international conference on computer vision*, 13189–13198.
- Wang, X.; Ang Jr, M. H.; and Lee, G. H. 2020. Cascaded refinement network for point cloud completion. In *Proceedings of the IEEE/CVF Conference on Computer Vision and Pattern Recognition*, 790–799.
- Wang, Y.; Sun, Y.; Liu, Z.; Sarma, S. E.; Bronstein, M. M.; and Solomon, J. M. 2019b. Dynamic graph cnn for learning on point clouds. *Acm Transactions On Graphics (tog)*, 38(5): 1–12.
- Wen, X.; Xiang, P.; Han, Z.; Cao, Y.-P.; Wan, P.; Zheng, W.; and Liu, Y.-S. 2021. Pmp-net: Point cloud completion by learning multi-step point moving paths. In *Proceedings of the IEEE/CVF Conference on Computer Vision and Pattern Recognition*, 7443–7452.
- Wu, W.; Qi, Z.; and Fuxin, L. 2019. Pointconv: Deep convolutional networks on 3d point clouds. In *Proceedings of the IEEE/CVF Conference on Computer Vision and Pattern Recognition*, 9621–9630.
- Xiang, P.; Wen, X.; Liu, Y.-S.; Cao, Y.-P.; Wan, P.; Zheng, W.; and Han, Z. 2021. Snowflakenet: Point cloud completion by snowflake point deconvolution with skip-transformer. In *Proceedings of the IEEE/CVF International Conference on Computer Vision*, 5499–5509.
- Xie, H.; Yao, H.; Zhou, S.; Mao, J.; Zhang, S.; and Sun, W. 2020. Grnet: Gridding residual network for dense point cloud completion. In *Computer Vision—ECCV 2020: 16th European Conference, Glasgow, UK, August 23–28, 2020, Proceedings, Part IX*, 365–381. Springer.
- Yan, X.; Yan, H.; Wang, J.; Du, H.; Wu, Z.; Xie, D.; Pu, S.; and Lu, L. 2022. Fbnet: Feedback network for point cloud completion. In *Computer Vision—ECCV 2022: 17th European Conference, Tel Aviv, Israel, October 23–27, 2022, Proceedings, Part II*, 676–693. Springer.
- Yang, Y.; Feng, C.; Shen, Y.; and Tian, D. 2018. Foldingnet: Point cloud auto-encoder via deep grid deformation. In *Proceedings of the IEEE Conference on Computer Vision and Pattern Recognition*, 206–215.
- Yu, X.; Rao, Y.; Wang, Z.; Liu, Z.; Lu, J.; and Zhou, J. 2021. Point: Diverse point cloud completion with geometry-aware transformers. In *Proceedings of the IEEE/CVF International Conference on Computer Vision*, 12498–12507.
- Yuan, W.; Khot, T.; Held, D.; Mertz, C.; and Hebert, M. 2018. Pcn: Point completion network. In *2018 International Conference on 3D Vision (3DV)*, 728–737. IEEE.
- Zhang, S.; Liu, X.; Xie, H.; Nie, L.; Zhou, H.; Tao, D.; and Li, X. 2023a. Learning geometric transformation for point cloud completion. *International Journal of Computer Vision*, 131(9): 2425–2445.
- Zhang, Z.; Dong, B.; Li, T.; Heide, F.; Peers, P.; Yin, B.; and Yang, X. 2023b. Single Depth-image 3D Reflection Symmetry and Shape Prediction. In *Proceedings of the IEEE/CVF International Conference on Computer Vision*, 8896–8906.
- Zhao, H.; Jiang, L.; Jia, J.; Torr, P. H.; and Koltun, V. 2021. Point transformer. In *Proceedings of the IEEE/CVF international conference on computer vision*, 16259–16268.
- Zhao, H.; Wei, S.; Shi, D.; Tan, W.; Li, Z.; Ren, Y.; Wei, X.; Yang, Y.; and Pu, S. 2023. Learning symmetry-aware geometry correspondences for 6D object pose estimation. In *Proceedings of the IEEE/CVF International Conference on Computer Vision*, 14045–14054.
- Zhou, H.; Cao, Y.; Chu, W.; Zhu, J.; Lu, T.; Tai, Y.; and Wang, C. 2022. Seedformer: Patch seeds based point cloud completion with upsample transformer. In *Computer Vision—ECCV 2022: 17th European Conference, Tel Aviv, Israel, October 23–27, 2022, Proceedings, Part III*, 416–432. Springer.
- Zhou, Y.; Liu, S.; and Ma, Y. 2021. NeRD: Neural 3d reflection symmetry detector. In *Proceedings of the IEEE/CVF Conference on Computer Vision and Pattern Recognition*, 15940–15949.
- Zhu, Z.; Chen, H.; He, X.; Wang, W.; Qin, J.; and Wei, M. 2023. SVDFormer: Complementing Point Cloud via Self-view Augmentation and Self-structure Dual-generator. In *Proceedings of the IEEE/CVF International Conference on Computer Vision*, 14508–14518.

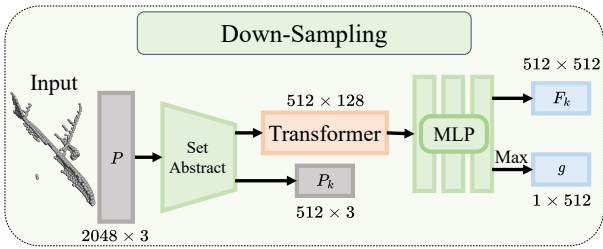


Figure 9: The detailed architecture of our Down-sampling module in the Local Symmetry Transformation Network (LSTNet). The “Max” is the max-pooling operation.

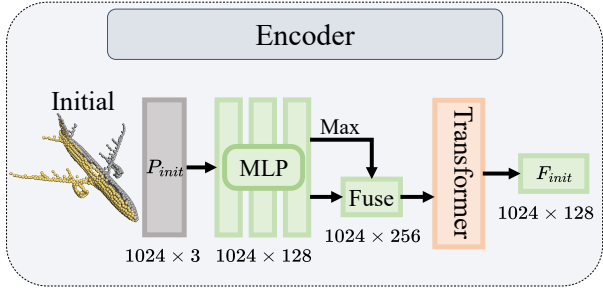


Figure 10: The detailed architecture of our Encoder in the Symmetry-Guide Transformer (SGFormer). The “Max” is the max-pooling operation.

Appendix

Detailed Architecture

In this section, we present the detailed architecture of our down-sampling module in LSTNet and our encoder in SGFormer, including the number of points and channels for each module.

As shown in Figure 9, our Down-sampling module utilizes set abstraction (Qi et al. 2017b) to obtain down-sampled point clouds P_k with 512 points and features with 128 dimensions. We then apply the point transformer (Zhao et al. 2021) to gain local features and use several MLPs to expand channel dimensions, resulting in final local features F_k . Global features g are formed by leveraging a max-pooling operation.

As shown in Figure 10, our Encoder extracts point features and global features of input P_{init} using MLPs and the max-pooling operation. After fusing point features and global features by concatenation and MLPs, we apply the point transformer (Zhao et al. 2021) to obtain final point features F_{init} .

Implementation Details.

We utilized PyTorch and CUDA to construct our network and trained our models with an AdamW optimizer at a base learning rate of 0.0002. As shown in Figure 9 and Figure 10, in the initial stage, our approach involves obtaining key points and corresponding key features with 512 points and 512 channels, respectively. Note that, the 128-dimensional feature after the Transformer layer is fed into the refinement

Local features	Global awareness	CD (\downarrow)	F1 (\uparrow)
✓		6.41	0.846
	✓	6.49	0.842
✓	✓	6.28	0.853

Table 7: Ablation of local feature and global awareness in terms of l_1 Chamfer Distance $\times 10^3$ (CD) and F1-Score@%1 (F1) on PCN dataset.

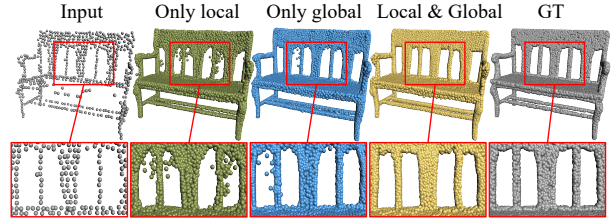


Figure 11: Visualized comparison for dual-path perception in our SGFormer.

stage as the feature of partial point clouds. In the refinement stage, the number of feature channels of feature F_{init} is 128. Before fusing feature F_{init} with the feature F_k and feature F_m , we leverage MLPs to expand their channels from 128 to 256, resulting in a final feature F'_{init} with 512 channels. In addition, the number of attention heads in all attention blocks is 4 and we stack two cascaded SGFormer to refine initial point clouds gradually.

Extra Ablation Studies

In this section, we provide extra ablation studies for our SymmCompletion.

Ablation for LSTNet. In this section, we explore the design of our Local Symmetry Transformation Network (LSTNet). As we mentioned in the manuscript, we leverage both global and local features of partial inputs to achieve our local symmetry. The quantitative comparison of the global and local features is reported in Table 7. We can find that the setting of both global and local features obtain the best performance. We argue that global awareness helps to predict highly accurate point-wise symmetry by recognizing the global structure and topology of partial inputs. As shown in Figure 11, using global and local features together produces smoother results than using them alone. In addition, we replaced the initial point cloud generation models of other models with our LSTNet to validate the effectiveness of our point-wise symmetry transformations. The quantitative comparison results are shown in Table 8. As we can see, after replacing with our LSTNet, the performances of both SnowflakeNet (Xiang et al. 2021) and SVDFormer (Zhu et al. 2023) improved significantly.

Ablation for SGFormer. In the refinement stage, previous methods proposed many impressive approaches to form fine-grained completion results. In this ablation study, we explore the performance between previous refinement networks and our Symmetry-Guide Transformer (SGFormer). We choose three recent methods to compare, including SnowflakeNet (Xiang et al. 2021) (SPD module), Seed-

Initial method	SnowflakeNet	SVDFormer
Vanilla	7.21	6.54
LSTNet	6.92	6.47

Table 8: Comparison between our LSTNet and previous initial point cloud generation networks in terms of $l1$ Chamfer Distance $\times 10^3$ on PCN dataset.

Methods	SPD	UpFormer	SDG	SGFormer
CD (\downarrow)	7.15	6.87	6.49	6.28
F1 (\uparrow)	0.799	0.812	0.840	0.853

Table 9: Comparison between our SGFormer and previous refinement networks in terms of $l1$ Chamfer Distance $\times 10^3$ (CD) and F1-Score@%1 (F1) on PCN dataset.

Former (Zhou et al. 2022) (UpFormer module), and SVDFormer (Zhu et al. 2023) (SDG module). In particular, we use these modules to replace our SGFormer. The quantitative and qualitative comparisons are shown in Table 9, our SGFormer achieves the best performance compared with previous refinement networks. Due to the introduction of symmetry guidance, SGFormer obtains a series of symmetric information to enhance the perception of discontinuous and holey regions in initial point clouds. However, previous methods refine initial point clouds based on only their geometric structures, making it difficult for them to complete these discontinuous and holey regions. As shown in Figure 12, previous refinement networks fail to solve a large hole in the partial input. In contrast, our SGFormer generates a complete and accurate shape consistent with the ground-truth point clouds.

Complexity analysis.

In this analysis, we compare the complexity and efficiency between recent methods and our SymmCompletion in Table 10, where results are tested on the PCN dataset. For a fair comparison, we test computation complexity (FLOPs), number of parameters (Params), and inference time (Time) on the same device with a single NVIDIA GTX 4090 GPU. The comparison demonstrates that SymmCompletion achieves the best performance in terms of completion accuracy and speed.

Visualization analysis and limitation

In this section, we provide a detailed visualized analysis to indicate our completion process. Then, we study our limitations based on these analyses.

Firstly, we visualize the regular completion process of our SymmCompletion. As shown in Figure 13, we first gain the missing parts based on local symmetry and then obtain the initial point clouds, in which we can find several noticeable hollow and discontinuous regions. However, this problem is solved by our optimization network SGFormer progressively. This visualization indicates the effectiveness of our SymmCompletion to achieve high-fidelity and high-consistency results.

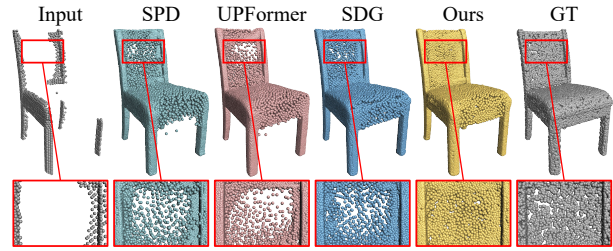


Figure 12: Visualized comparison for different refinement modules.

Secondly, because our LSTNet exploits the symmetry attribute to form missing parts, we provided an additional completion process for those special asymmetric cases. As shown in Figure 14, our LSTNet tends to reconstruct overall point clouds rather than only missing parts when meeting the asymmetric situation. The reason is that our local symmetry is achieved by point-wise affine and translation transformation. The local translation transformation enhances the model’s robustness for solving these asymmetric cases. In addition, our SGFormer is also able to help recover these asymmetric cases because the features of partial inputs are provided to our optimization process. In short, our approach also can complete asymmetric shapes.

Although our model achieved state-of-the-art performance, it struggles to accurately reconstruct the true appearance of objects in some challenging inputs, particularly those lacking symmetry as shown in Figure 15. It is worth noting that this is a common challenge for all point cloud completion methods, and our method forms better results than previous methods. For example, in the bottom case of Figure 15, our SymmCompletion generates more accurate and smoother missing parts based on symmetry information compared to existing methods. In future research, we plan to enhance the network’s ability to complete those challenging inputs by introducing other priors, such as the visual or geometric priors from large models.

More visualized results

We present additional visualized results on PCN dataset (Figure 16 and Figure 17), KITTI dataset (Figure 18), MVP dataset (Figure 19), and ShapeNet55 dataset (Figure 20) to demonstrate the high-quality and high-fidelity completion of our SymmCompletion. For MVP and ShapeNet55 datasets, we show mirror point clouds, initial point clouds, and two refined results (Fine1 and Fine2).

Methods	FLOPs (G)	#Params (M)	Time (ms)	CD (\downarrow)
Pointr(Yu et al. 2021)	18.81	30.10	15.43	8.38
SeedFormer (Zhou et al. 2022)	107.51	3.31	16.50	6.74
AnchorFormer (Chen et al. 2023b)	14.54	30.46	23.71	6.59
SVDFormer (Zhu et al. 2023)	50.14	30.75	17.09	6.54
SymmCompletion	22.60	6.64	13.24	6.28

Table 10: Comparison between our SymmCompletion and the most current methods on effectiveness and efficiency.

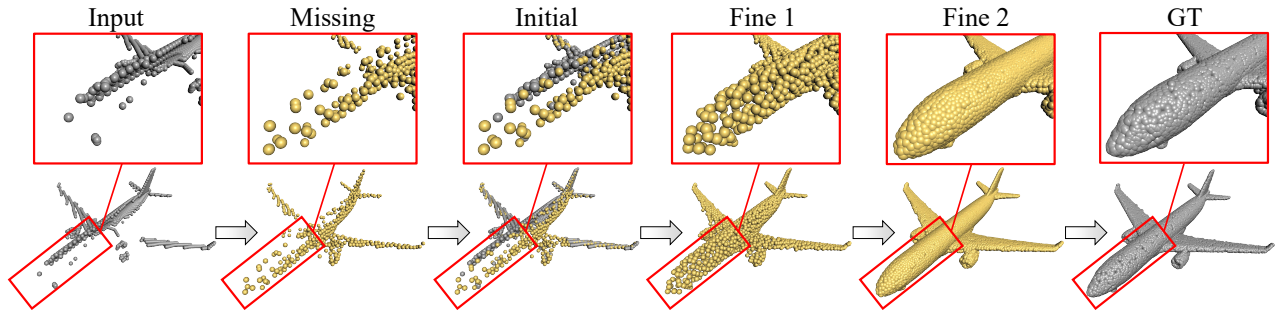


Figure 13: Visualized completion process of our SymmCompletion.

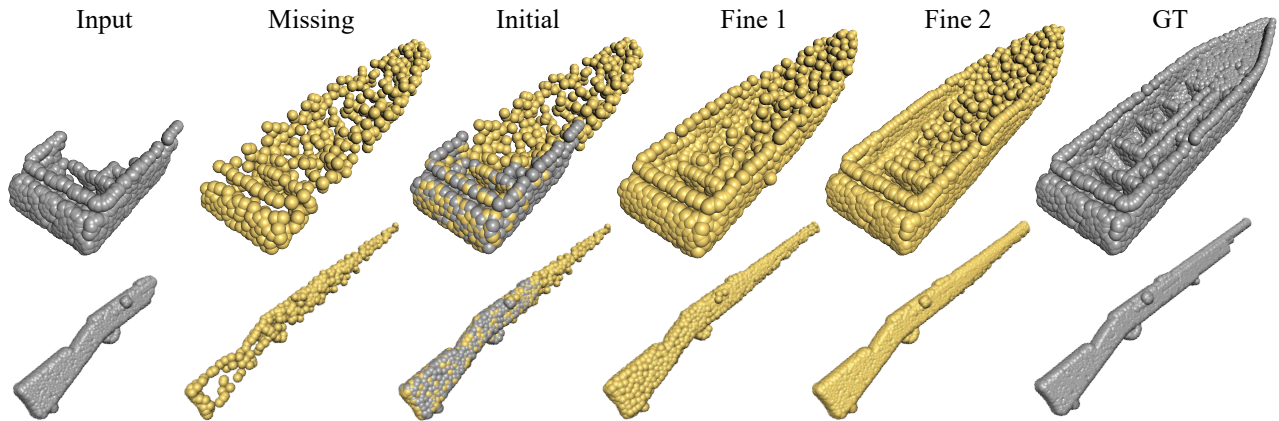


Figure 14: Example of Asymmetric cases.

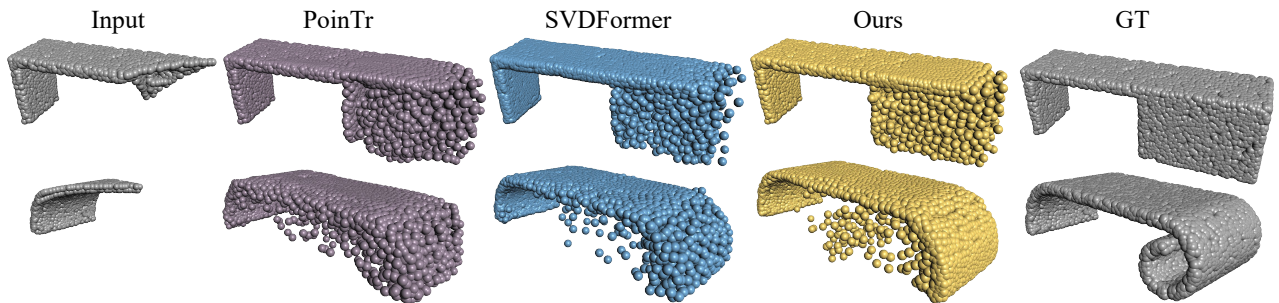


Figure 15: Example of failure cases.

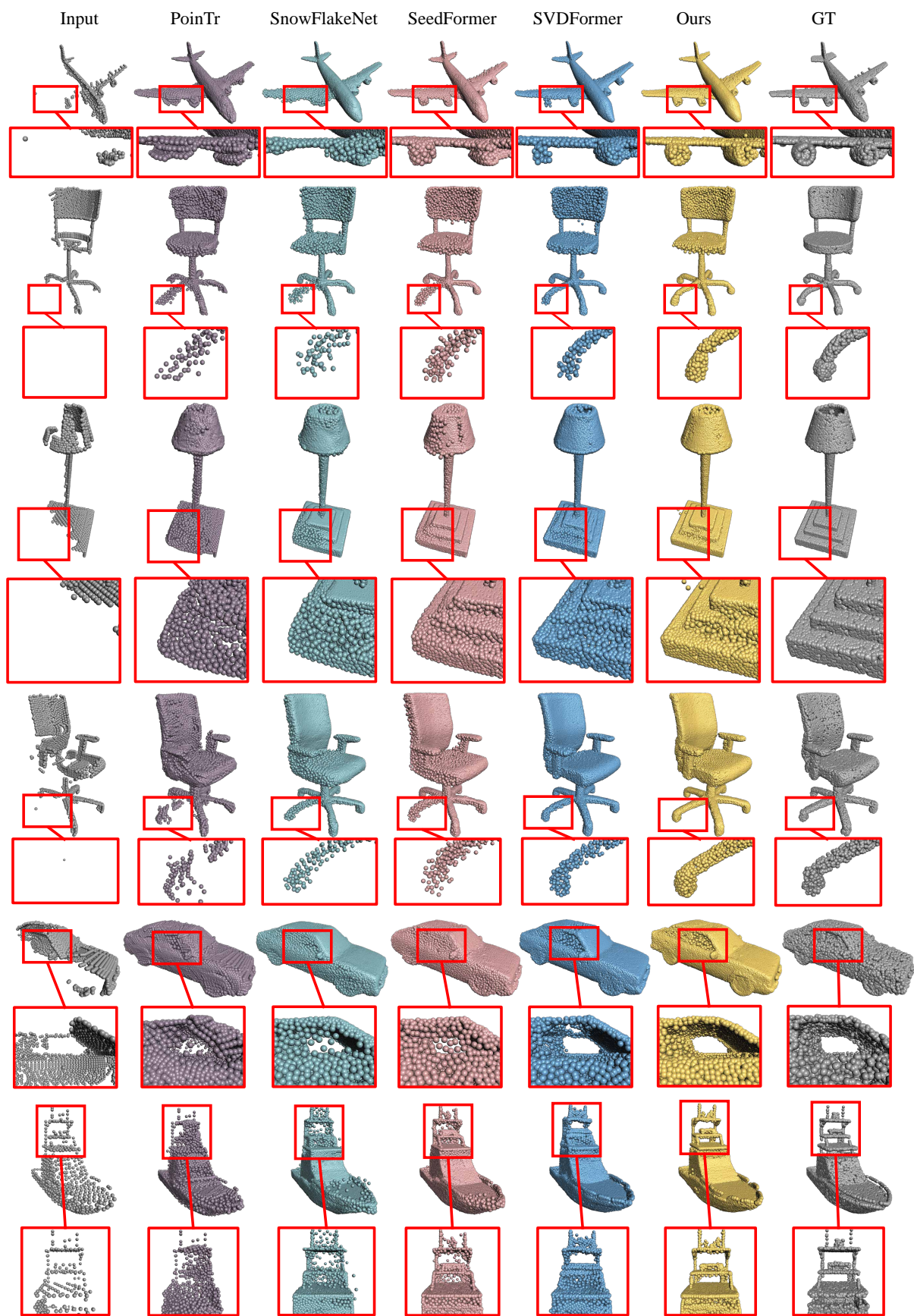


Figure 16: The extra visualized results on the PCN dataset.

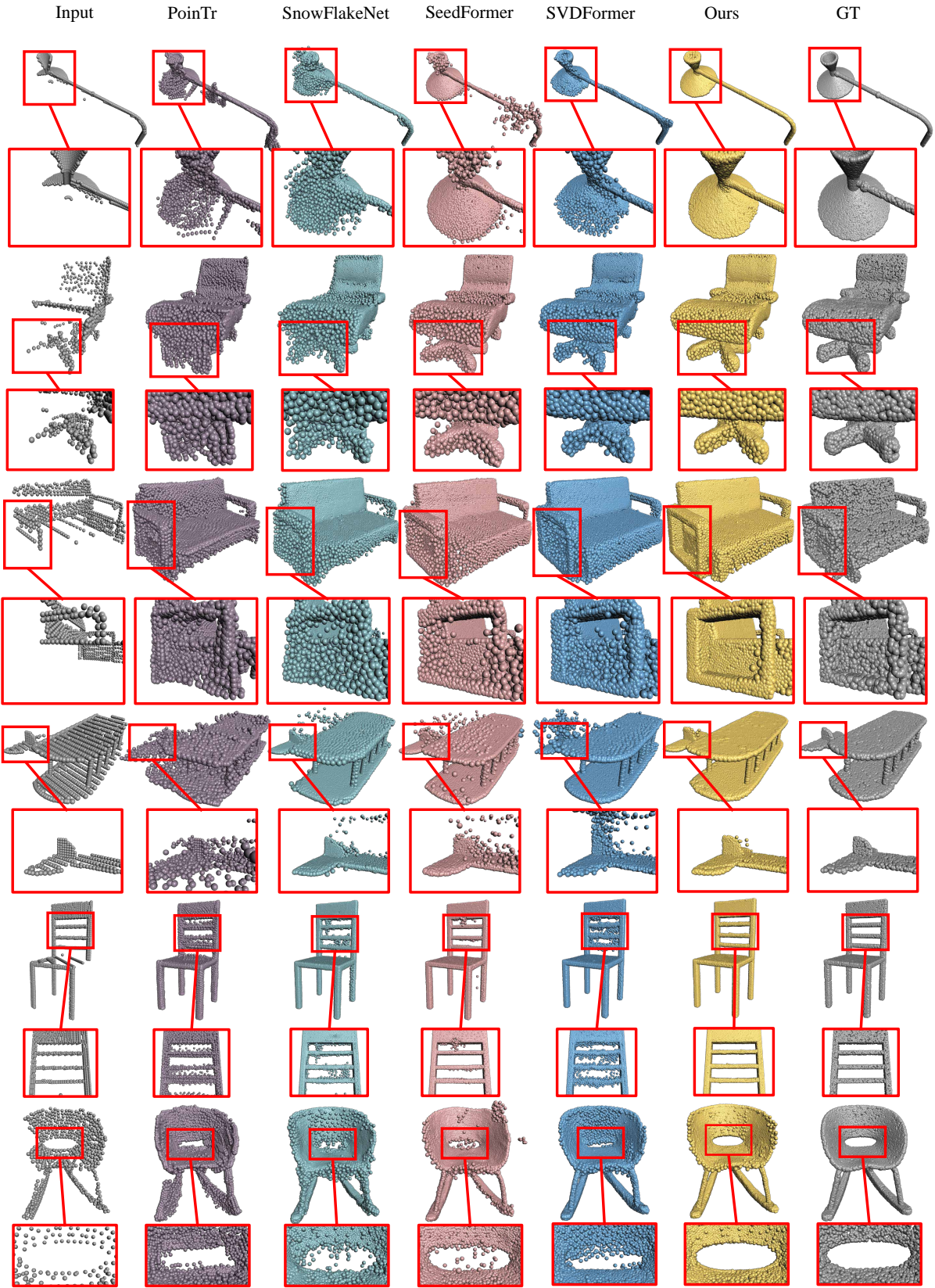


Figure 17: The extra visualized results on the PCN dataset.

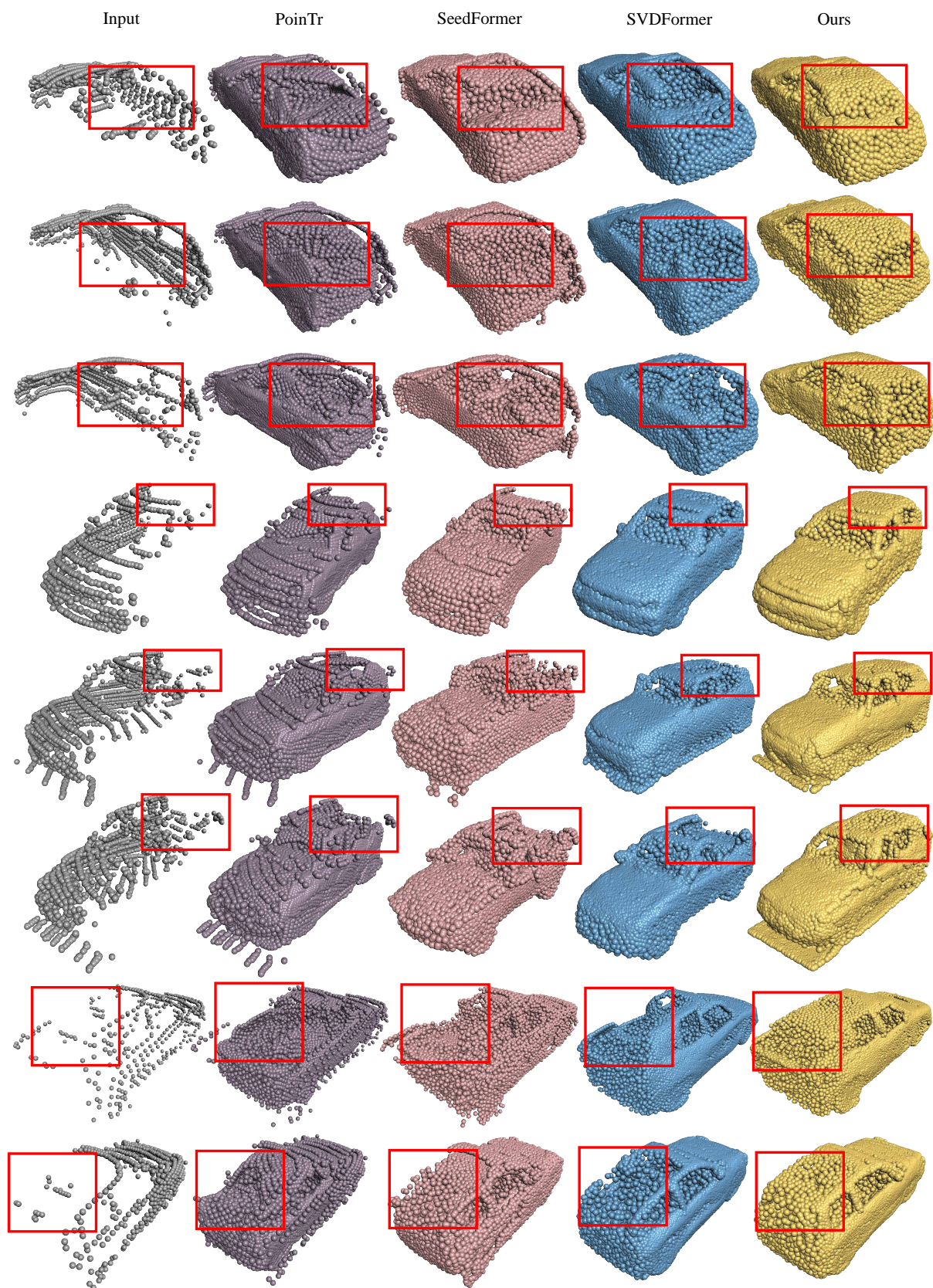


Figure 18: The extra visualized results on the KITTI dataset.

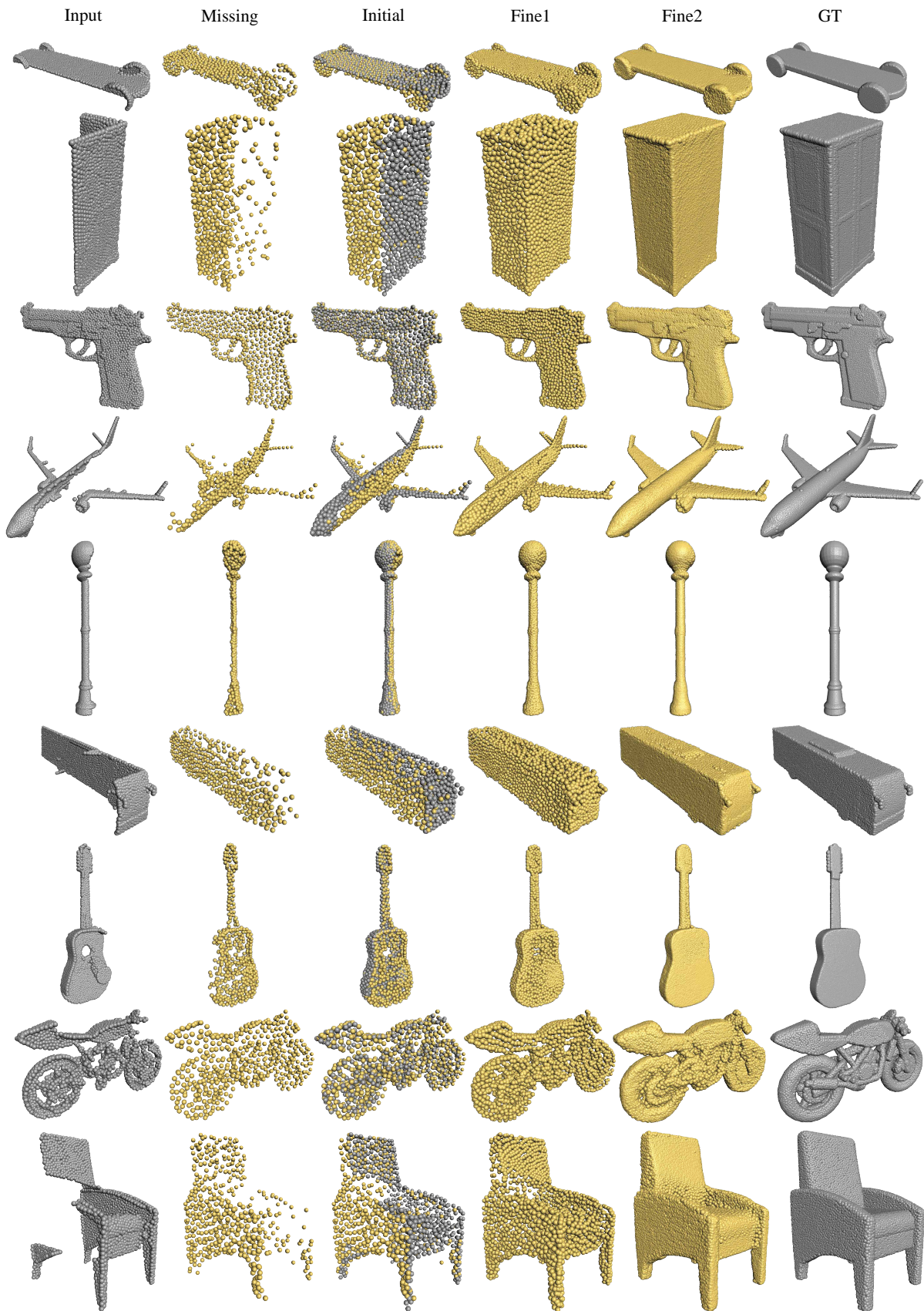


Figure 19: The visualized results of our SymmCompletion on the MVP dataset.

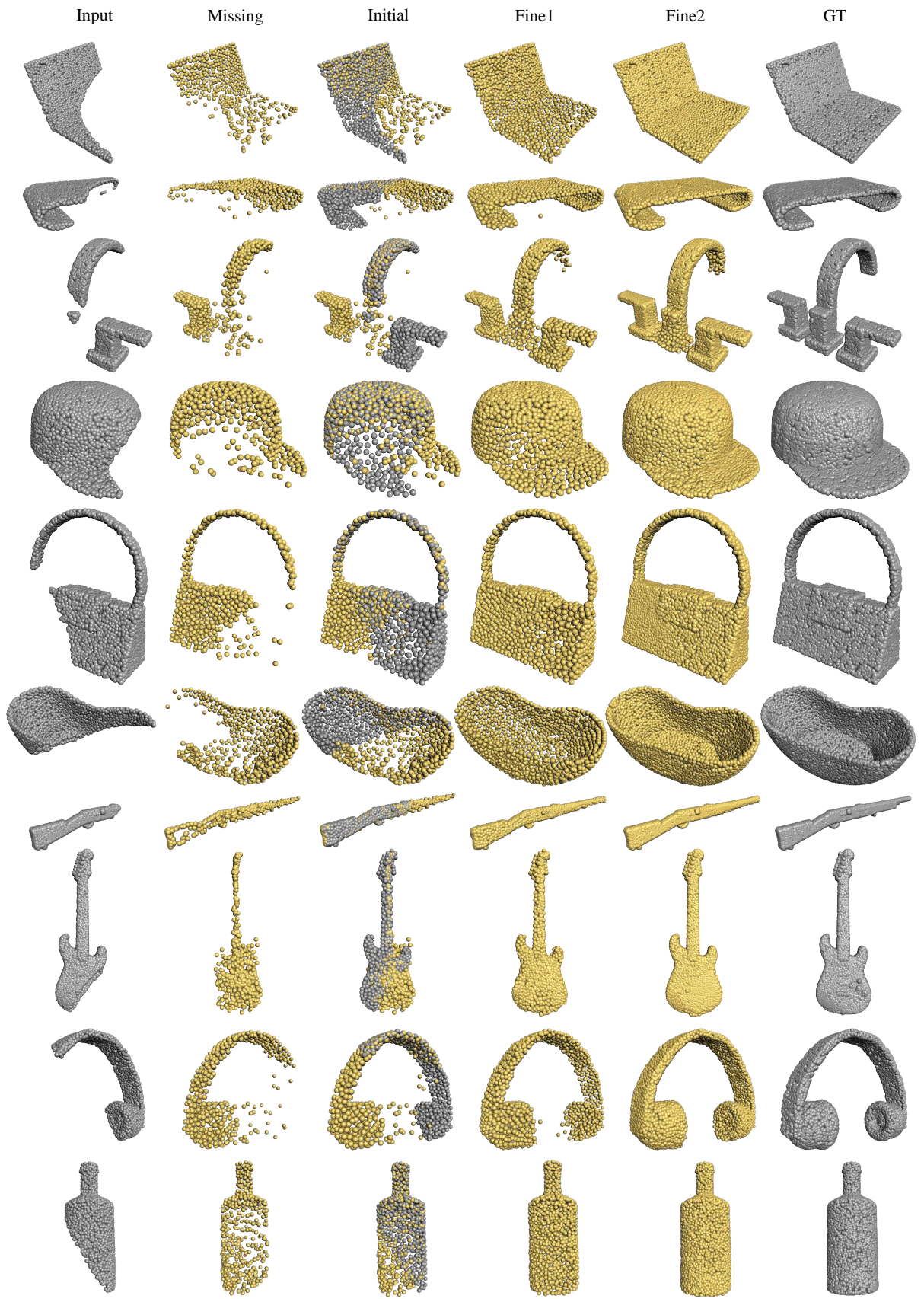


Figure 20: The visualized results of our SymmCompletion on the ShapeNet dataset.